

# Velocity-Space Contours of Collision Integrals

R. Narasimha,<sup>1</sup> S. M. Deshpande,<sup>1</sup>  
and P. V. Subba Raju<sup>1</sup>

*Received October 23, 1969*

---

Based on the recently found closed-form expressions of the Boltzmann collision integrals in a rigid-sphere gas for multi-Maxwellian distributions, a few typical sets of contour surfaces of the integrals in the space of molecular velocities are presented. These show graphically the tendency toward equilibrium under the influence of collisions. A brief preliminary comparison with Monte Carlo results is also given.

---

**KEY WORDS:** Kinetic theory of gases; Boltzmann equation; collision integrals; nonequilibrium in hard-sphere gases; numerical analysis of collision integrals; exact results for collision integrals.

## 1. INTRODUCTION

It has recently been shown (1-3) that, when the distribution function in a gas is "multi-Maxwellian" (i.e., can be expressed as a linear combination of Maxwellians), the computation of the Boltzmann collision integrals becomes feasible, and indeed that, for a rigid-sphere gas, the results can be expressed in closed form. This provides us for the first time with some exact results in situations involving large departures from equilibrium. The difficulties involved in evaluating the collision integrals in general have encouraged, on the one hand the use of outright hypotheses on their structure (as, e.g., in the well-known relaxation models), and on the other hand the development of purely numerical methods, especially Monte Carlo techniques.<sup>(4,5)</sup> An assessment of the BGK model based on these exact results has already been given.<sup>(3)</sup> The purpose of this note is to present some representative velocity-space contours of the collision integrals for a Mott-Smith bimodal distribution, with a view to illustrating graphically how collisions take a distribution toward equilibrium, and also to enable a direct comparison with the interesting computations made by the Monte Carlo group at Illinois,<sup>(5,6)</sup> which are the only other results available on

---

<sup>1</sup> Department of Aeronautical Engineering, Indian Institute of Science, Bangalore, India.

the collision integrals. A fairly extensive analysis of both random and systematic errors in such Monte Carlo work has been undertaken over a period of years,<sup>(7)</sup> but it has had to rely on purely numerical methods. The present results could, we believe, provide a more direct basis for such investigations.

## 2. THE CLOSED-FORM EXPRESSIONS

Details of the analysis leading to the closed-form expressions have been published elsewhere<sup>(1-3)</sup>; we only mention here the final result.

If the distribution function can be expressed as a weighted sum of Maxwellians  $F_i$ ,

$$f = \sum_i \nu_i F_i$$

$$F_i = n_i (\beta_i / \pi)^{3/2} \exp[-\beta_i (\mathbf{v} - \mathbf{u}_i)^2]$$

$$\equiv n_i (\beta_i / \pi)^{3/2} \exp(-\mathcal{C}_i^2)$$
(1)

where  $n_i$ ,  $\beta_i$ , and  $\mathbf{u}_i$  are the parameters in  $F_i$ , then the Boltzmann collision integrals can be written as

$$\mathcal{J}(f, f) = \sum_i \sum_j \nu_i \nu_j \mathcal{J}(F_i, F_j)$$
(2)

For rigid spheres of diameter  $\sigma$ , it has been shown that

$$\mathcal{J}(F_i, F_j) = (\pi^2 \sigma^2 / \beta_i \beta_j) F_i F_j [(1/2R) \{ \Phi(1; \frac{1}{2}; Q + R) - \Phi(1; \frac{1}{2}; Q - R) \}$$

$$- 2(\beta_i / \beta_j) \Phi(2; \frac{3}{2}; \mathcal{C}_j^2)]$$
(3)

where

$$Q = \frac{1}{2}(\mathcal{C}_i^2 + \mathcal{C}_j^2), \quad R^2 = \frac{1}{4}(\mathcal{C}_i^2 - \mathcal{C}_j^2) + |\mathcal{C}_i \times \mathcal{C}_j|^2$$

and the  $\Phi$  represent confluent hypergeometric functions (see Ref. 3). Thus, the calculation of  $\mathcal{J}$  requires only the evaluation of the relevant hypergeometric functions. A simple computer program has been written for doing this; high accuracy can easily be achieved (eight figures in the present work) using the well-known series representation for  $\Phi$  when the argument is less than 10, and an asymptotic expansion when the argument is larger.<sup>(8)</sup> It must be emphasized that no numerical quadrature is necessary at any stage for computing the collision integrals for rigid spheres. (Work now in progress indicates, however, that, for other intermolecular force models, at least one numerical integration may be necessary.)

## 3. RESULTS

Using the program mentioned above, we have, for purposes of illustration, computed the collision integrals in a few different cases for a Mott-Smith type of distribution

$$f_0 = (1 - \nu) F_1 + \nu F_2$$
(4)

where  $F_1$  and  $F_2$  are the Maxwellian distributions corresponding to the equilibrium states of a monatomic gas respectively on the cold and hot sides of a normal shock.

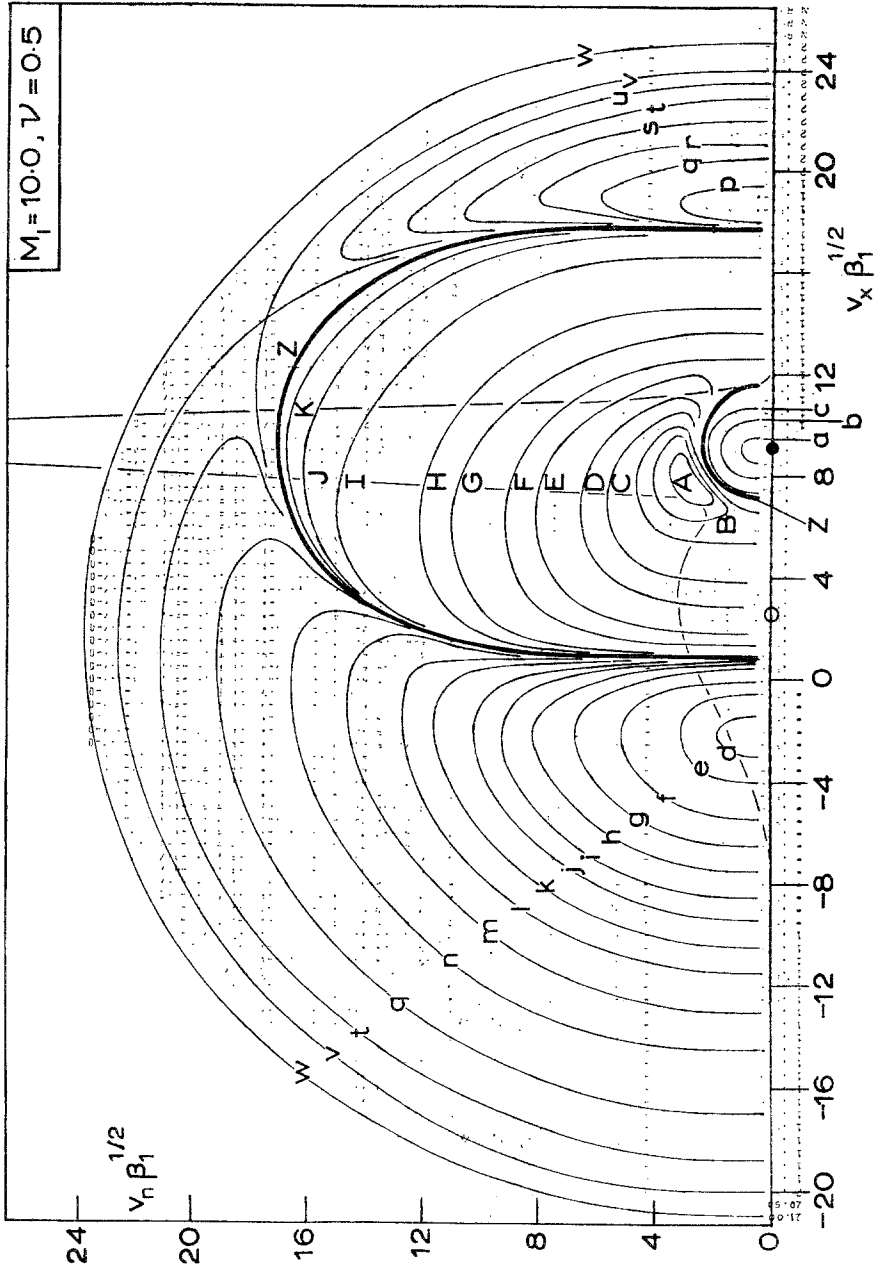


Fig. 1. Contours in velocity space of the collision integrals  $\mathcal{J}$  for a Mott-Smith distribution at  $M_1 = 10.0$ ,  $\nu = 0.5$ . The curve in the background represents the distribution function in  $v_x$ ,  $f_0(v_x, v_n = 0)$ . The two symbols on the  $v_x$ -axis mark the gas velocities  $u_1$  (filled circle) and  $u_2$  (open circle). The labels on the contours denote intervals in values of  $\mathcal{J}$  as given in Table I.

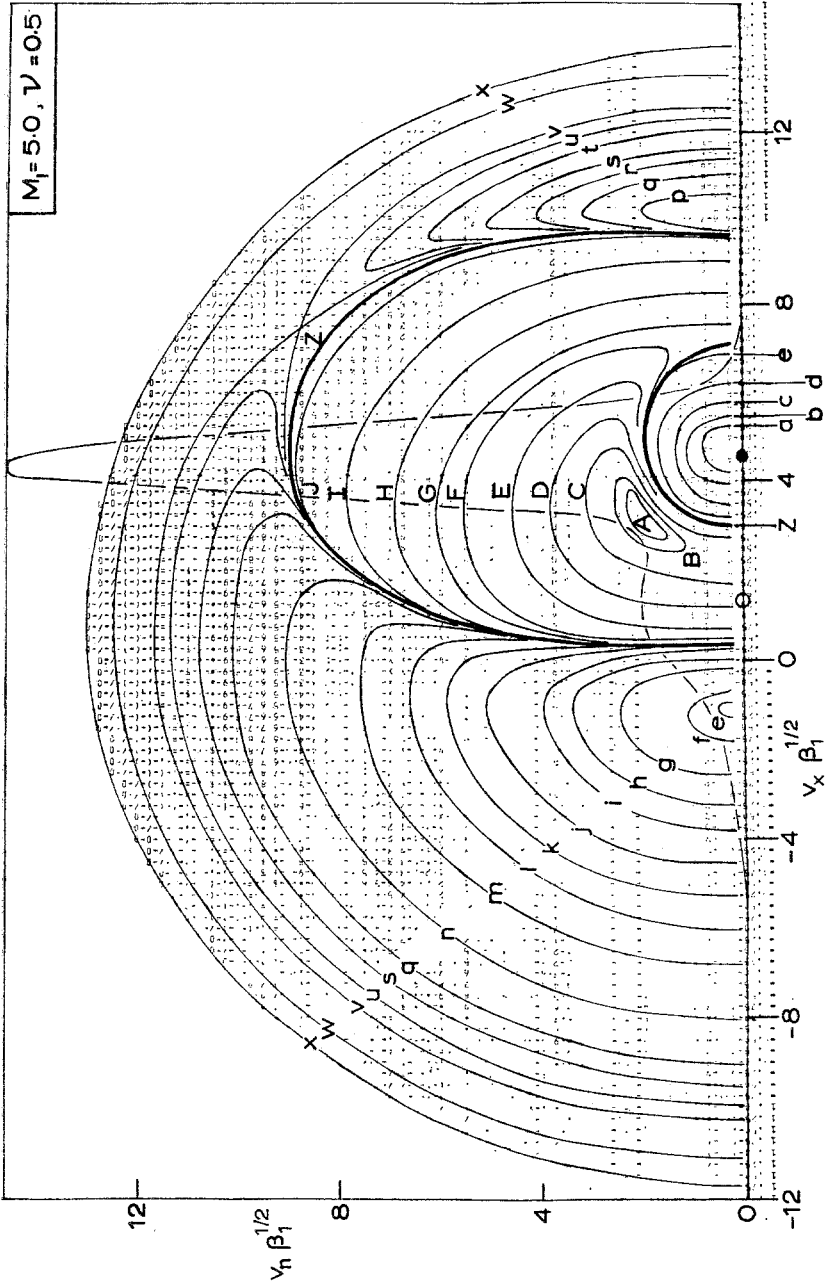


Fig. 2. Collision integral contours for Mott-Smith distribution at  $M_1 = 5.0$ ,  $\nu = 0.5$ . Notation is the same as in Fig. 1 except for the labels on the contours, which now denote intervals as shown in Table II.

Table I. Intervals in Values of  $\mathcal{J}$  for Fig. 1<sup>a</sup>

4.8	<	<i>A</i>	<	$6.0 \times 10^{-2}$	-4.7	<	<i>a</i>	<	-2.7
3.9		<i>B</i>		$4.8 \times 10^{-2}$	-2.7		<i>b</i>		-1.5
3.1		<i>C</i>		$3.9 \times 10^{-2}$	-0.29		<i>c</i>		-0.16
2.0		<i>D</i>		$2.5 \times 10^{-2}$	-1.0		<i>d</i>		$-0.83 \times 10^{-2}$
0.52		<i>E</i>		$0.65 \times 10^{-2}$	-0.83		<i>e</i>		$-0.69 \times 10^{-2}$
0.27		<i>F</i>		$0.33 \times 10^{-2}$	-0.58		<i>f</i>		$-0.44 \times 10^{-2}$
0.75		<i>G</i>		$1.1 \times 10^{-3}$	-0.34		<i>g</i>		$-0.26 \times 10^{-2}$
0.22		<i>H</i>		$0.34 \times 10^{-3}$	-0.20		<i>h</i>		$-0.16 \times 10^{-2}$
0.91		<i>I</i>		$1.6 \times 10^{-5}$	-1.2		<i>i</i>		$-0.92 \times 10^{-3}$
0.86		<i>J</i>		$1.6 \times 10^{-6}$	-0.71		<i>j</i>		$-0.54 \times 10^{-3}$
0.15		<i>K</i>		$0.27 \times 10^{-6}$	-0.33		<i>k</i>		$-0.25 \times 10^{-3}$
					-0.15		<i>l</i>		$-0.11 \times 10^{-3}$
					-0.67		<i>m</i>		$-0.30 \times 10^{-4}$
					-1.3		<i>n</i>		$-0.59 \times 10^{-5}$
					-0.26		<i>p</i>		$-0.12 \times 10^{-5}$
					-1.2		<i>q</i>		$-0.51 \times 10^{-6}$
					-0.51		<i>r</i>		$-0.23 \times 10^{-6}$
					-0.23		<i>s</i>		$-0.10 \times 10^{-6}$
					-1.0		<i>t</i>		$-0.45 \times 10^{-7}$
					-0.45		<i>u</i>		$-0.20 \times 10^{-7}$
					-2.0		<i>v</i>		$-0.89 \times 10^{-8}$
					-0.4		<i>w</i>		$-0.18 \times 10^{-8}$

<sup>a</sup> Mott-Smith distribution at  $M_1 = 10.0$ ,  $\nu = 0.5$ . Values in units of  $n$ ,  $\beta$ ,  $\sigma^2$ .

Table II. Intervals in Values of  $\mathcal{J}$  for Fig. 2<sup>a</sup>

0.96	<	<i>A</i>	<	$1.1 \times 10^{-1}$	-2.0	<	<i>a</i>	<	-1.4
0.87		<i>B</i>		$0.96 \times 10^{-1}$	-1.4		<i>b</i>		-0.9
0.57		<i>C</i>		$0.79 \times 10^{-1}$	-0.6		<i>c</i>		-0.4
0.29		<i>D</i>		$0.40 \times 10^{-1}$	-1.8		<i>d</i>		$-1.2 \times 10^{-1}$
0.11		<i>E</i>		$0.15 \times 10^{-1}$	-2.9		<i>e</i>		$-2.6 \times 10^{-2}$
0.27		<i>F</i>		$0.38 \times 10^{-2}$	-2.6		<i>f</i>		$-2.4 \times 10^{-2}$
0.12		<i>G</i>		$0.18 \times 10^{-2}$	-2.4		<i>g</i>		$-1.5 \times 10^{-2}$
0.24		<i>H</i>		$0.36 \times 10^{-3}$	-1.5		<i>h</i>		$-0.94 \times 10^{-2}$
0.32		<i>I</i>		$0.47 \times 10^{-4}$	-9.4		<i>i</i>		$-5.9 \times 10^{-3}$
0.38		<i>J</i>		$0.67 \times 10^{-6}$	-3.7		<i>j</i>		$-2.3 \times 10^{-3}$
					-1.4		<i>k</i>		$-0.9 \times 10^{-3}$
					-5.6		<i>l</i>		$-3.5 \times 10^{-4}$
					-1.4		<i>m</i>		$-0.85 \times 10^{-4}$
					-1.6		<i>n</i>		$-0.91 \times 10^{-5}$
					-0.3		<i>p</i>		$-0.17 \times 10^{-5}$
					-1.7		<i>q</i>		$-0.97 \times 10^{-6}$
					-0.97		<i>r</i>		$-0.55 \times 10^{-6}$
					-0.55		<i>s</i>		$-0.28 \times 10^{-6}$
					-0.28		<i>t</i>		$-0.14 \times 10^{-6}$
					-1.4		<i>u</i>		$-0.69 \times 10^{-7}$
					-0.69		<i>v</i>		$-0.35 \times 10^{-7}$
					-0.87		<i>w</i>		$-0.43 \times 10^{-8}$
					-0.22		<i>x</i>		$-0.11 \times 10^{-8}$

<sup>a</sup> Mott-Smith distribution at  $M_1 = 5.0$ ,  $\nu = 0.5$ . Values in units of  $n$ ,  $\beta$ ,  $\sigma^2$ .

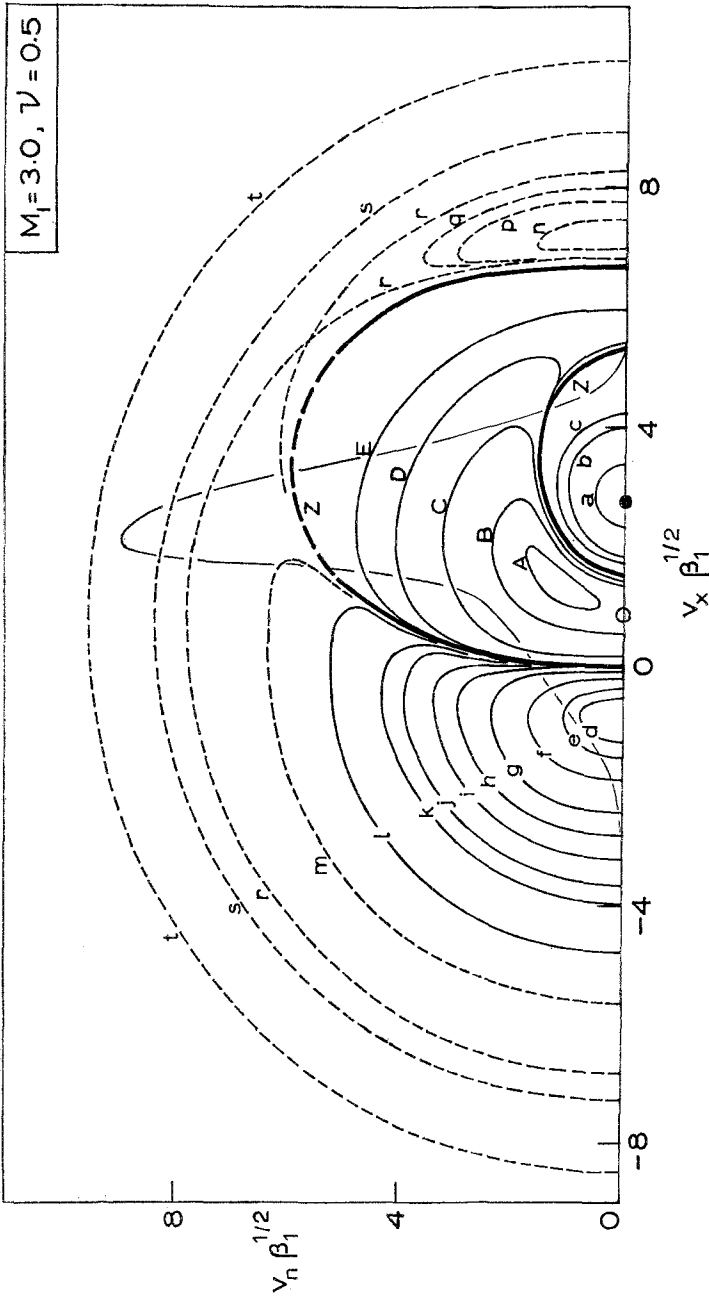


Fig. 3. Collision integral contours for Mott-Smith distribution at  $M_1 = 3.0$ ,  $\nu = 0.5$ . Notation is the same as before except for the labels on the contours, which now denote values (on full lines) and intervals (on dashed lines) as in Table III.

Table III. Values of  $\mathcal{J}$  and Intervals for Fig. 3<sup>a</sup>

<i>A</i>	0.09	<i>a</i>	-0.6
<i>B</i>	0.05	<i>b</i>	-0.2
<i>C</i>	$10^{-2}$	<i>c</i>	-0.1
<i>D</i>	$10^{-3}$	<i>d</i>	$-3.5 \times 10^{-2}$
<i>E</i>	$10^{-4}$	<i>e</i>	$-3.0 \times 10^{-2}$
		<i>f</i>	$-2.0 \times 10^{-2}$
		<i>g</i>	$-1.0 \times 10^{-2}$
		<i>h</i>	$-0.5 \times 10^{-2}$
		<i>i</i>	$-0.25 \times 10^{-2}$
		<i>j</i>	$-0.10 \times 10^{-2}$
		<i>k</i>	$-5.0 \times 10^{-4}$
		<i>l</i>	$-0.5 \times 10^{-4}$
		<i>m</i>	$-3.8 \times 10^{-6}$
		<i>n</i>	$-0.7 \times 10^{-6}$
		<i>p</i>	$-2.3 \times 10^{-7}$
		<i>q</i>	$-1.3 \times 10^{-7}$
		<i>r</i>	$-4.3 \times 10^{-8}$
		<i>s</i>	$-4.5 \times 10^{-9}$
		<i>t</i>	$-1.7 \times 10^{-11}$

<sup>a</sup> Mott-Smith distribution at  $M_1 = 3.0$ ,  $\nu = 0.5$ . Values in units of  $n$ ,  $\beta$ ,  $\sigma^2$ .

The results are available in the form of tables<sup>2</sup> if accurate numerical values are desired, but are otherwise most conveniently displayed in the form of contours in velocity space, of the kind shown by Nordsieck and Hicks.<sup>(5)</sup> Because of the symmetry of the distribution (4) about the  $v_x$  axis ( $v_x$  being the component of the molecular velocity along the flow direction  $x$ ), it is enough in this case to show a section of the contour surfaces in  $\mathbf{v}$ -space by a plane through the  $v_x$  axis ( $v_n$  being the normal coordinate in this plane). Such contours can effectively be produced by the computer itself, if suitable format instructions are incorporated in the program. Figures 1 and 2 show contours obtained this way; the lines shown have been drawn in on the computer sheets, joining printout symbols representing the same interval of  $\mathcal{J}$ . The labels on the curves stand for intervals in values of  $\mathcal{J}$  as shown in the Tables I and II.

Although this method of obtaining contours is the most convenient, its accuracy is limited by the number of symbols available on the printer and certain other similar considerations. In one case, we have used a more accurate "manual" procedure, in which the contours have been drawn by interpolating among the values of  $\mathcal{J}$  computed on a fine grid in velocity space. The results obtained this way are shown as full lines in Fig. 3 (see Table III for appropriate values); the dashed lines in this diagram have again been obtained directly from the computer.

These diagrams show vividly how collisions tend to drive a system toward equilibrium. Comparison with the corresponding distribution function (whose shape at  $v_n = 0$  is displayed in the background in all the three diagrams) shows that in

<sup>2</sup> Available on request from the authors.

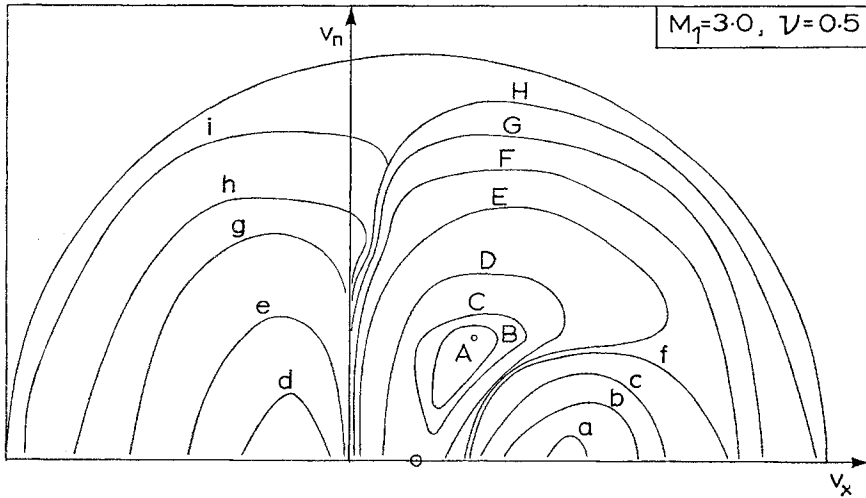


Fig. 4. Collision integral contours for the same distribution as in Fig. 3, as obtained from one Monte Carlo run (Yen, private communication). Average contour values, in arbitrary units, are given in Table IV.

each case there is a loss of molecules ( $\mathcal{J} < 0$ ) from the supersonic “peak” (i.e., the region in velocity space around  $v_x \simeq u_1$ , the gas velocity on the supersonic side of the shock), and also from the region corresponding roughly to  $v_x < 0$  (i.e., to molecules coming from the hot side). In between is a region where the gain predominates ( $\mathcal{J} > 0$ ). The general tendency therefore is (as might be expected) to level down the peaks and fill up the valleys in the distribution.

Recalling that the diagrams show a section of the contour surfaces in  $\mathbf{v}$ -space, we can describe the results in greater detail as follows. There is a ball (or, more precisely, a spheroidal shape) roughly around the supersonic gas velocity on the cold side, in which the loss predominates ( $\mathcal{J} < 0$ ). This is surrounded by a region, contained within an oblate spheroidal shape, in which the gain predominates ( $\mathcal{J} > 0$ ). Between these two surfaces (marked  $Z$  in the diagrams),  $\mathcal{J}$  attains a maximum value on some ring (within the surface marked  $A$ ). Beyond the second spheroid  $Z$ ,  $\mathcal{J}$  is again negative and eventually approaches zero at large velocities.

Table IV. Average Contour Values (in arbitrary units) for Fig. 4

$A$	$175 \times 10^{-5}$	$a$	$-1000 \times 10^{-5}$
$B$	$130 \times 10^{-5}$	$b$	$-500 \times 10^{-5}$
$C$	$100 \times 10^{-5}$	$c$	$-200 \times 10^{-5}$
$D$	$50 \times 10^{-5}$	$d$	$-50 \times 10^{-5}$
$E$	$10 \times 10^{-5}$	$e$	$-25 \times 10^{-5}$
$F$	$3 \times 10^{-5}$	$f$	$-10 \times 10^{-5}$
$G$	$1 \times 10^{-5}$	$g$	$-6 \times 10^{-5}$
		$h$	$-2 \times 10^{-5}$
		$i$	0



To enable a comparison with Monte Carlo results, we reproduce the contours obtained by Yen in Fig. 4 (see Table IV for appropriate values), which can be directly compared with Fig. 3, as both computations are for the same distribution.<sup>3</sup> It is interesting that many of the gross features of  $\mathcal{J}$  are reasonably well displayed by the Monte Carlo results. A detailed numerical comparison is not immediately possible, because the normalization used in the Monte Carlo results is not accurately known. However, even a cursory comparison reveals certain qualitative features which may need improvement in the Monte Carlo results. We may mention the shape of the zero lines ( $Z$  in our diagrams), the slope of the contours as they come in toward the  $v_x$  axis, and the presence of saddle points at large velocities.

## ACKNOWLEDGMENTS

We thank Prof. S. M. Yen for kindly furnishing copies of Fig. 4, and some other results of his unpublished computations. The work reported here has been supported by a grant from the Aeronautical Research Committee of the Council for Scientific and Industrial Research.

## REFERENCES

1. R. Narasimha and S. M. Deshpande, "The Boltzmann collision integrals, I. General analysis," Aeronautical Research Committee (India) ARC-TN-1 (1968).
2. S. M. Deshpande and R. Narasimha, "The Boltzmann collision integrals, II. Rigid spheres," Aeronautical Research Committee (India) ARC-TN-2 (1969).
3. S. M. Deshpande and R. Narasimha, "The Boltzmann collision integrals for a combination of Maxwellians," *J. Fluid Mech.* **36**:545 (1969).
4. G. A. Bird, "The velocity distribution function within a shock wave," *J. Fluid Mech.* **30**:479 (1967).
5. A. Nordsieck and B. L. Hicks, "Monte Carlo evaluation of the Boltzmann collision integrals," *Proc. 5th Intl. Symp. on Rarefied Gas Dynamics*, Oxford, Vol. 1, p. 695 (Academic Press, New York, 1967).
6. S. M. Yen and B. L. Hicks, "On the accuracy of approximate solutions of the Boltzmann equations," *Proc. 5th Intl. Symp. on Rarefied Gas Dynamics*, Oxford, Vol. 1, p. 695 (Academic Press, New York, 1967).
7. B. L. Hicks and M. A. Smith, "Numerical studies of strong shock waves. Part X: On the accuracy of Monte Carlo solutions of the nonlinear Boltzmann equation," Rep. R-360, Coordinated Science Laboratory, University of Illinois (1967).
8. A. Erdelyi *et al.*, *Higher Transcendental Functions*, Vol. 2 (McGraw-Hill, New York, 1953).
9. R. Narasimha and S. M. Deshpande, "On the accuracy of Monte Carlo computations of the Boltzmann collision integrals," Report 68 FM3, Department of Aeronautical Engineering, Indian Institute of Science, Bangalore, India (1968).

<sup>3</sup> Prof. Yen has informed us that Fig. 2 of Ref. 5 is wrongly captioned, and is not a plot of contours of  $\mathcal{J}$  but of  $v_n \mathcal{J}$ . Comments made in an earlier report<sup>(9)</sup> therefore need to be modified slightly as here.